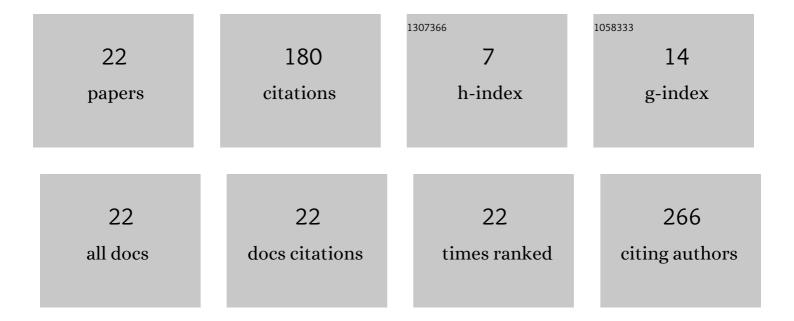
## Eugenio Torres-GarcÃ-a

List of Publications by Year in descending order

Source: https://exaly.com/author-pdf/1607480/publications.pdf

Version: 2024-02-01



#	Article	IF	CITATIONS
1	Preclinical evaluation of early multi-organ toxicity induced by liposomal doxorubicin using <sup>67</sup> Ga-citrate. Nanotoxicology, 2022, 16, 247-264.	1.6	4
2	Determination of experimental Cherenkov spectrum (200–1050 nm) of <sup>18</sup> F and its implications on optical dosimetry: murine model. Radiation Effects and Defects in Solids, 2022, 177, 869-879.	0.4	1
3	Femur absorptiometry changes determined by X-ray image segmentation in mice under experimental diabetes and ovariectomy. Applied Radiation and Isotopes, 2021, 170, 109608.	0.7	1
4	Evaluation of doxorubicin-induced early multi-organ toxicity in male CD1 mice by biodistribution of <sup>18</sup> F-FDG and <sup>67</sup> Ga-citrate. Pilot study. Toxicology Mechanisms and Methods, 2021, 31, 546-558.	1.3	4
5	Professional and academic follow up of 100+ graduates of the UAEMex-ININ masters and doctorate program in medical physics in Mexico. AIP Conference Proceedings, 2021, , .	0.3	0
6	Effects of chronic immobilization stress on biokinetics and dosimetry of 67Ga in a murine model. Radiation and Environmental Biophysics, 2020, 59, 257-263.	0.6	1
7	Differences in the S value between male and female murine model for diagnostic, therapeutic and theragnostic radionuclides. Applied Radiation and Isotopes, 2019, 146, 61-65.	0.7	2
8	Theoretical and experimental characterization of emission and transmission spectra of Cerenkov radiation generated by 177Lu in tissue. Journal of Biomedical Optics, 2019, 24, 1.	1.4	7
9	New track-structure Monte Carlo code for 4D ionizing photon transport. Radiation Effects and Defects in Solids, 2018, 173, 567-577.	0.4	0
10	A new Monte Carlo code for light transport in biological tissue. Medical and Biological Engineering and Computing, 2018, 56, 649-655.	1.6	6
11	67 Ga as a biosensor of iron needs in different organs: Study performed on male and female rats subjected to iron deficiency and exercise. Journal of Trace Elements in Medicine and Biology, 2017, 44, 93-98.	1.5	3
12	Dose per unit cumulated activity (S-values) for eâ^' and beta emitting radionuclides in cancer cell models calculated by Monte Carlo simulation. Applied Radiation and Isotopes, 2014, 90, 229-233.	0.7	7
13	Monte Carlo mitochondrial dosimetry and microdosimetry of 1311. Radiation Protection Dosimetry, 2013, 153, 411-416.	0.4	3
14	Multifunctional targeted therapy system based on <sup>99m</sup> Tc/ <sup>177</sup> Luâ€labeled gold nanoparticlesâ€Tat(49–57)â€Lys <sup>3</sup> â€bombesin internalized in nuclei of prostate cancer cells. Journal of Labelled Compounds and Radiopharmaceuticals, 2013, 56, 663-671.	0.5	73
15	Multifunctional Targeted Radiotherapy System for Induced Tumours Expressing Gastrin-releasing Peptide Receptors. Current Nanoscience, 2012, 8, 193-201.	0.7	14
16	153Sm-HM for arthritic knee pain. Estimated dosimetry. Australasian Physical and Engineering Sciences in Medicine, 2012, 35, 63-69.	1.4	0
17	Specific energy from Auger and conversion electrons of1311,188Re-anti-CD20 to a lymphocyte's nucleus. Radiation Effects and Defects in Solids, 2011, 166, 40-43.	0.4	1
18	Effect of chemical composition and density of the pelvic structure in intracavitary brachytherapy dosimetry. Radiation Physics and Chemistry, 2011, 80, 349-353.	1.4	1

#	Article	lF	CITATIONS
19	Biokinetics and Dosimetry of 188Re-anti-CD20 in Patients with Non-Hodgkin's Lymphoma: Preliminary Experience. Archives of Medical Research, 2008, 39, 100-109.	1.5	25
20	Biokinetics and dosimetry of target-specific radiopharmaceuticals for molecular imaging and therapy. Radiation Effects and Defects in Solids, 2007, 162, 785-789.	0.4	0
21	Monte Carlo microdosimetry of188Re- and131I-labelled anti-CD20. Physics in Medicine and Biology, 2006, 51, N349-N356.	1.6	11
22	An efficient, reproducible and fast preparation of 188Re-anti-CD20 for the treatment of non-Hodgkin's lymphoma. Nuclear Medicine Communications, 2005, 26, 793-799.	0.5	16